Event-Based State Estimation with Variance-Based Triggering

Sebastian Trimpe and Raffaello D'Andrea

***Abstract*— An event-based state estimation scenario is considered where a sensor sporadically transmits observations of a scalar linear process to a remote estimator. The remote estimator is a time-varying Kalman filter. The triggering decision is based on the estimation variance: the sensor runs a copy of the remote estimator and transmits a measurement if the associated measurement prediction variance exceeds a tolerable threshold. The resulting variance iteration is a new type of Riccati equation with switching that corresponds to the availability or unavailability of a measurement and depends on the variance at the previous step. We study asymptotic properties of the variance iteration and, in particular, asymptotic convergence to a periodic solution.**

I. Introduction

We study the recursive equation

$$p(k+1) = a^2\, p(k) + q - \gamma(p(k))\, \frac{a^2\, c^2\, p^2(k)}{c^2\, p(k) + r} \tag{1}$$

$$p(0) = p_0 \geq 0, \tag{2}$$

with the switching function

$$\gamma(p(k)) := \begin{cases} 1 & \text{if } c^2(p(k) - \bar{p}) \geq \delta \\ 0 & \text{otherwise} \end{cases} \tag{3}$$

and parameters $|a| > 1$, $c \neq 0$, $q > 0$, $r > 0$, $\delta > 0$. The equation represents the iteration of the prediction variance for the event-based remote state estimation problem depicted in Fig. 1. The remote estimator is a time-varying Kalman filter, $p(k)$ is the state prediction variance, and (3) is the triggering rule used by the sensor: a measurement is transmitted if, and only if, the prediction variance grows too large. The details of the derivation of (1) (including the explanation of the additional parameter $\bar{p}$) are deferred to Sec. II.

The main result of this paper is to prove the global convergence of the iteration (1) to a periodic solution under certain assumptions to be derived herein as well. To the authors' knowledge, the discrete-time Riccati-type iteration (1) has not been studied before.

Implementing a copy of the remote estimator on the sensor node to decide whether or not to transmit data as shown in Fig. 1 makes sense, for example, when the process is to be monitored from a remote location, and communication is expensive compared to local processing on the sensor. The problem considered herein is a special case of a more general problem that we are interested in. We consider the networked control system (NCS) in Fig. 2, where multiple agents observe and act on a dynamic system, and share data with each other over a broadcast network. Each agent's objective is to maintain an estimate of the full system state $x(k)$ (for example, to feed its local controller). Since the state may not be observable from a local sensor alone, communication between the agents is required. By *reduced communication state estimation* we mean: the problem of maintaining an estimate of the system state on each agent of an NCS while, at the same time, seeking to reduce the load on the communication network.

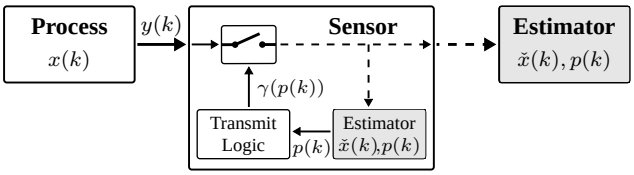

Fig. 1. Event-based state estimation problem. A sensor observes a linear process with state $x(k)$ and transmits measurements $y(k)$ sporadically over a network link to a remote estimator, which keeps track of the conditional state mean $\check{x}(k)$ and variance $p(k)$. The sensor implements a copy of the remote estimator and uses its variance $p(k)$ to make the transmit decision. Solid lines denote continuous flow of data (at every time step of the underlying discrete-time sampling) and dashed lines indicate discontinuous data flow. The communication links are assumed ideal (no delays or packet drops).

Figure 3 explains an event-based strategy to address this problem. The key idea is that each agent broadcasts its local sensor measurement to the other agents only *if it is required in order to meet a certain estimation performance*. To be able to make this decision, each agent implements a copy of the common estimator representing the common information in the network. If the other agents' estimate (represented by the common estimator) of a particular measurement is already "good enough," it is not required to communicate this measurement. This scheme has been experimentally demonstrated on the Balancing Cube, [1], to achieve significant reduction in average communication rates, [2], [3].

Different decision rules for considering an estimate "good enough" can be implemented in the transmit logic block. In [2], a constant threshold logic on the difference of the actual measurement and its prediction by the common estimator is implemented. In [3], a measurement is broadcast if its prediction variance exceeds a tolerable bound. This is also the approach taken in this paper. If a transmission is triggered by a condition on the estimation variance, we refer to this as *variance-based triggering*. While [3] presents purely experimental results, the theoretical basis of the approach is developed herein.

The problem scenario in Fig. 1 is recovered from the

S. Trimpe and R. D'Andrea are with the Institute for Dynamic Systems and Control (IDSC), ETH Zurich, Sonneggstr. 3, 8092 Zurich, Switzerland {strimpe, rdandrea}@ethz.ch.

Accepted final version. To appear in *Proc. of the 51st IEEE Conference on Decision and Control, 2012*.

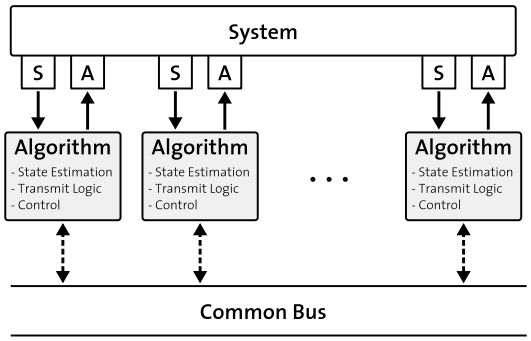

Fig. 2. Networked control system. Multiple sensor (S) and actuator (A) units are spatially distributed along a dynamic system. Each sensor and actuator is associated with an algorithm block; and sensor, actuator, and algorithm together are denoted as an *agent*. The agents can share data over a common bus. In order to feed its local controller, each agent maintains an estimate of the full system state x. Each agent also decides when to share its local sensor data with its peers over the common bus.

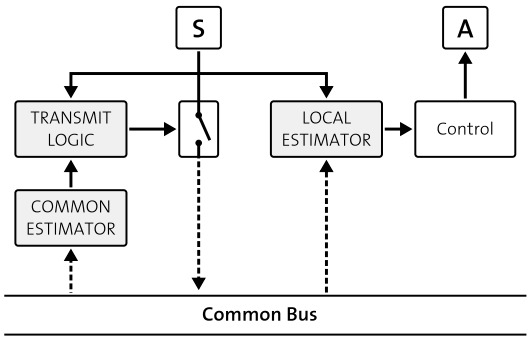

Fig. 3. Event-based strategy to reduced communication state estimation. The drawing represents a single agent (sensor (S), actuator (A), algorithm) of Fig. 2. Each agent implements a copy of the *common estimator*, which operates on data that is received over the common bus. Since all agents have access to this data, the estimators are identical and represent the common information in the network. Data from the common estimator is used in some *transmit logic* (event generator) to decide whether or not to put the local sensor data on the bus. This allows an efficient use of the communication resource: an agent's measurement is broadcast to all other agents only if the common estimate of this measurement is not already satisfactory (measured, for example, by its variance). A second estimator, the *local estimator*, may be used to exploit all sensor data that is locally available, i.e. the data received from the bus *and* the local sensor data. Its estimate is used for feedback control.

one in Fig. 2 when only two agents are considered, one of which observes the system through its local sensor and sporadically transmits data to the other, which estimates the system state based on this information. The common estimator then corresponds to the remote estimator in Fig. 1. Equation (1) is, in fact, the scalar version of the matrix variance iteration derived in [3] for the distributed event-based estimation problem of Fig. 2 and 3.

For the specific problem in [3], convergence of the estimation variance iteration to a periodic solution was observed to numerical accuracy. This observation motivates the theoretical study of the convergence properties of the event-based state estimator with variance-based triggering in this paper. To focus on the fundamental properties, this paper deals with the scalar problem.

A. Related work

Event-based strategies are a popular means of ensuring efficient use of the communication resource in NCS (see [4] and references therein). As opposed to traditional time-triggered transmission of data, event-based approaches transmit data only when required to meet a certain specification of the control system (e.g. closed-loop stability, control or estimator performance). Event-based state estimation problems with a single sensor and a single estimator node similar to Fig. 1 have been studied in [4]–[11], for example. Event-based state estimation problems for distributed or multi-agent systems have been looked at in [2], [3], [12].

In most of the above-mentioned references for the single sensor/single estimator case, the sensor node transmits to the remote estimator a local state estimate (obtained from a Kalman filter on the sensor) rather than the raw measurement. While this seems to be the method of choice for the single agent case (the state estimate contains the fused information of all past measurements), communicating raw measurements has a practical advantage for the multi-agent case. For an agent to fuse another agent's measurement with its local state estimate, it needs to know the variance of the measurement conditioned on the state. This is usually known in form of a sensor model. To optimally fuse another agent's state estimate, on the other hand, the variance associated with the estimate would have to be known. Since this variance is, however, only known to the agent that generated the estimate, it would have to be communicated over the network as well, hence, increasing the network load.

In the above-mentioned references on event-based estimation, an event is triggered by some condition on real-time data (measurement or state); that is, in a stochastic framework, data transmission is a random event. In contrast, the variance-based trigger in (3) depends on the prediction variance at the previous step. The resulting variance iteration (1) is deterministic and depends on the problem data only. A condition on the variance to trigger sensor transmissions is considered in [13] in a slightly different framework. Therein, the authors consider two heterogeneous sensors: at every time step, one of these transmits its measurement to a remote estimator, and a condition on the estimator variance is used to decide which one. Whereas in that scenario, the average communication rate is constant, we seek to reduce the average sensor transmission rate, including the case where no data is transmitted at a time step.

The variance iteration of other Kalman filtering problems (their scalar version) can be recovered from (1) by replacing $\gamma(p(k))$ in (1) with:

- $\gamma(k) = 1$. Classic Kalman filter for linear time-invariant systems, [14]. The filter has access to a measurement at every time step. Iteration (1) is called the *discrete-time Riccati equation*, [14]. It is well known that it converges to a positive fixed point for the assumed parameters.
- $\gamma(k) \in \{0, 1\}$ a periodic sequence. With periodic measurement transmissions, the problem can be modeled as linear periodic system with periodically varying

$c(k)$ and $r(k)$. The variance evolves according to the *discrete-time periodic Riccati equation*, whose convergence properties to periodic solutions are studied in [15]. The problem considered herein is different in that we do not assume a-priori a periodic transmit sequence.

- $\gamma(k) \in \{0, 1\}$ a Bernoulli random process. Kalman filtering with intermittent observations, [16]. The arrival of a measurement at the Kalman filter is subject to random data loss modeled as a Bernoulli process. Hence, $p(k)$ becomes a random variable. In [16], the authors show there exists a critical value for the data loss probability, below which the expected value of $p(k)$ is finite.

B. Outline of this paper

Equation (1) is formally derived in Sec. II. Section III illustrates the behavior of (1) with simulation examples. The asymptotic properties of (1) are studied in Sec. IV, and the main result of this paper is derived (Theorem 2). Due to space limitation, proofs of intermediate propositions have been omitted and will be published elsewhere; they are available in [17]. The paper concludes with a discussion in Sec. V.

II. Event-Based Kalman Filter

In this section, we derive (1) as the variance update of the event-based state estimator in Fig. 1 for a scalar linear stochastic process. A matrix version of this equation for a vector system with multiple sensors is derived in [3].

Consider the scalar stochastic linear time-invariant process

$$x(k+1) = a\,x(k) + v(k) \tag{4}$$

$$y(k) = c\,x(k) + w(k), \tag{5}$$

where k is the discrete-time index, $x(k)$ represents the process state, and $y(k)$ its observation. The process noise $v(k)$, the measurement noise $w(k)$, and the initial state $x(0)$ are assumed mutually independent, Gaussian distributed with mean 0, 0, x_0 and variance $q > 0$, $r > 0$, and $p_0 \geq 0$, respectively. For the purpose of this paper, we consider the case of unstable dynamics, i.e. $|a| > 1$, which is the more challenging case, since communication of measurements is required for the estimation error variance to be bounded. Furthermore, we assume that the system is detectable, i.e. $c \neq 0$.

It is well known that the Kalman filter, [14], is the optimal state estimator for the process (4), (5) in that it keeps track of the conditional probability distribution of the state $x(k)$ conditioned on all measurements up to time k, $\mathcal{Y}(k) := \{y(1), \ldots, y(k)\}$. To distinguish this Kalman filter from the reduced communication filter derived below, it is denoted as the *full communication Kalman filter*. Under the above assumptions, the state prediction variance $\mathrm{Var}\,[x(k)|\mathcal{Y}(k{-}1)]$ converges to $\bar{p} > 0$ which is the unique positive solution to the discrete algebraic Riccati equation (DARE)

$$\bar{p} = a^2\bar{p} + q - \frac{a^2c^2\bar{p}^2}{c^2\bar{p} + r}. \tag{6}$$

We write $\bar{p} = \mathrm{DARE}(a, c, q, r)$.

Next, we state the Kalman filter that estimates $x(k)$ based on a reduced set of measurements. Let $\tilde{\mathcal{Y}}(k)$ denote the collection of all measurements $y(k)$ up to time k that are available at the remote estimator,

$$\tilde{\mathcal{Y}}(k) := \{y(l) \mid l \leq k, \tilde{\gamma}(l) = 1\}, \tag{7}$$

where the transmit function $\tilde{\gamma}$ is defined as

$$\tilde{\gamma}(k) := \begin{cases} 1 & \text{if measurement } y(k) \text{ is transmitted} \\ 0 & \text{otherwise.} \end{cases} \tag{8}$$

Notice that, if the sequence of transmit decisions $\{\tilde{\gamma}(1), \ldots, \tilde{\gamma}(k)\}$ is known at time k, (7) is well defined. We make precise later in this section how we decide if a measurement is transmitted at time k.

Under the above assumptions, the distribution of the state $x(k)$ conditioned on $\tilde{\mathcal{Y}}(k)$ is Gaussian. The Kalman filter [14] keeps track of the conditional mean and variance,

$$\check{x}(k|k{-}1) = \mathrm{E}\,[x(k)|\tilde{\mathcal{Y}}(k{-}1)] \tag{9}$$

$$\check{x}(k|k) = \mathrm{E}\,[x(k)|\tilde{\mathcal{Y}}(k)] \tag{10}$$

$$p(k|k{-}1) = \mathrm{Var}\,[x(k)|\tilde{\mathcal{Y}}(k{-}1)] \tag{11}$$

$$p(k|k) = \mathrm{Var}\,[x(k)|\tilde{\mathcal{Y}}(k)], \tag{12}$$

where $\mathrm{E}\,[\cdot|\cdot]$ denotes the conditional expected value and $\mathrm{Var}\,[\cdot|\cdot]$ the conditional variance. The filter equations are

$$\check{x}(k|k{-}1) = a\,\check{x}(k{-}1|k{-}1) \tag{13}$$

$$p(k|k{-}1) = a^2\,p(k{-}1|k{-}1) + q \tag{14}$$

$$K(k) = \frac{c\,p(k|k{-}1)}{c^2\,p(k|k{-}1) + r} \tag{15}$$

$$\check{x}(k|k) = \check{x}(k|k{-}1) + \tilde{\gamma}(k)K(k)\big(y(k) - c\,\check{x}(k|k{-}1)\big) \tag{16}$$

$$p(k|k) = p(k|k{-}1) - \tilde{\gamma}(k)\,c\,K(k)\,p(k|k{-}1). \tag{17}$$

We denote the filter (13)–(17) as the *reduced communication Kalman filter*.

Let $p(k) := p(k|k{-}1)$ denote the state prediction variance. It captures the uncertainty about $x(k)$ given all measurements up to the previous time step $k{-}1$. Similarly, $\mathrm{Var}\,[y(k)|\tilde{\mathcal{Y}}(k{-}1)] = c^2p(k) + r$ captures the uncertainty in predicting the measurement $y(k)$. According to the idea outlined in the introduction, a measurement $y(k)$ is transmitted and used to update the estimator if, and only if, its prediction variance exceeds a tolerable bound. Since the reduced communication Kalman filter cannot do better than the full communication filter, we use a threshold δ on the difference

$$\mathrm{Var}\,[y(k)|\tilde{\mathcal{Y}}(k{-}1)] - \lim_{k\to\infty} \mathrm{Var}\,[y(k)|\mathcal{Y}(k{-}1)] = c^2(p(k) - \bar{p}) \tag{18}$$

for the transmit decision. Hence, we use the transmit rule

$$\tilde{\gamma}(k) = \gamma(p(k)) \tag{19}$$

with $\gamma(p(k))$ as in (3). We assume $\delta > 0$ henceforth; for $\delta = 0$, the full communication Kalman filter is recovered.

By combining equations (14), (15), (17), and (19), equation (1) is obtained.

III. Illustrative Examples

Figure 4(a) shows simulation results[1] of (1) for the following parameter values:

Example 1: $a = 1.2$, $c = q = r = 1$, $\delta = 3$, $p_0 = \bar{p}$.

As expected, the variance $p(k)$ grows at times where no measurement is available. Once the threshold is exceeded, a measurement is transmitted ($\gamma(p(k)) = 1$) and the estimator variance drops. The solution in Fig. 4(a) asymptotically converges to a periodic solution with period $N = 3$.

Figures 4(b) and 4(c) illustrate that, for different values of δ (all other parameters are the same as in Example 1), asymptotically periodic solutions with very different periods may be obtained. The period does not vary monotonically with δ.

IV. Asymptotic Convergence

The asymptotic properties of (1) are studied in this section. In particular, we derive conditions that guarantee convergence to a periodic solution and give an algorithm to compute the period. The convergence proof is based on the *contraction mapping theorem* (also known as *Banach's fixed point theorem*). After some preliminaries in Sec. IV-A, we use an illustrative example in Sec. IV-B to outline the convergence proof, which then follows in Sec. IV-C to IV-E.

A. Preliminaries

Since $q > 0$ and $r > 0$, (1) and (3) can equivalently be written as

$$\frac{p(k+1)}{q} = a^2 \frac{p(k)}{q} + 1 - \mathbf{1}_{\frac{p(k)}{q} - \frac{\bar{p}}{q} \geq \frac{\delta}{c^2 q}} \frac{a^2 \frac{c^2 q}{r} \left(\frac{p(k)}{q}\right)^2}{\frac{c^2 q}{r} \frac{p(k)}{q} + 1}, \quad (20)$$

where we use

$$\mathbf{1}_X := \begin{cases} 1 & \text{if } X \text{ is true} \\ 0 & \text{otherwise} \end{cases} \quad (21)$$

for a more compact notation. By redefining $p(k)$, c^2, and δ as $p(k)/q$, $c^2 q/r$, and $\delta/(c^2 q)$, respectively, we can assume without loss of generality that $q = r = 1$. Henceforth, we study the iteration

$$p(k+1) = h(p(k)), \quad p(0) = p_0 \geq 0, \quad (22)$$

where the function h is defined as

$$\begin{aligned} h \;:\; [0,\infty) &\to [0,\infty) \\ p &\mapsto a^2 p + 1 - \mathbf{1}_{p \geq \bar{p} + \delta} \frac{a^2 c^2 p^2}{c^2 p + 1} \end{aligned} \quad (23)$$

with parameters $|a| > 1$, $c \neq 0$, $\delta > 0$; and with $\bar{p} = \mathrm{DARE}(a, c, 1, 1)$. The graph of h is shown in Fig. 5 together with the graph of the function g,

$$\begin{aligned} g \;:\; [0,\infty) &\to [0,\infty) \\ p &\mapsto a^2 p + 1 - \frac{a^2 c^2 p^2}{c^2 p + 1}, \end{aligned} \quad (24)$$

[1]Files to run the simulation are available at www.cube.ethz.ch/downloads.

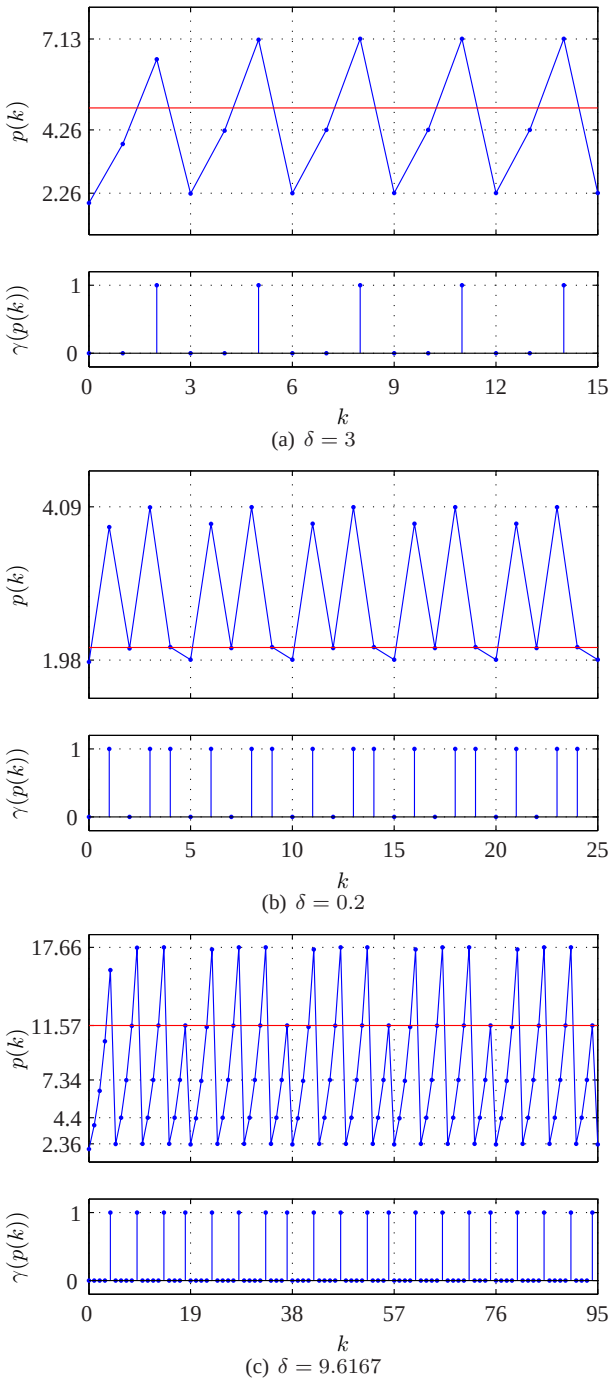

Fig. 4. Simulation results for different values of the threshold parameter δ. The top graph of each sub-figure shows the variance iterates $p(k)$ (blue) and the transmit threshold $\bar{p} + \delta/c^2$ (red). The bottom graph shows the corresponding transmit sequence $\gamma(p(k))$. All solutions are asymptotically periodic with periods $N = 3, 5, 19$ from top to bottom.

which represents the variance iteration of the full communication Kalman filter. For the map h being applied m times, we write h^m; that is, for $m \in \mathbb{N}$,

$$p(k+m) = h^m(p(k)) = \underbrace{h(h(\ldots(h}_{m}(p(k))\ldots))), \quad (25)$$

where $h^0(p(k)) := p(k)$.

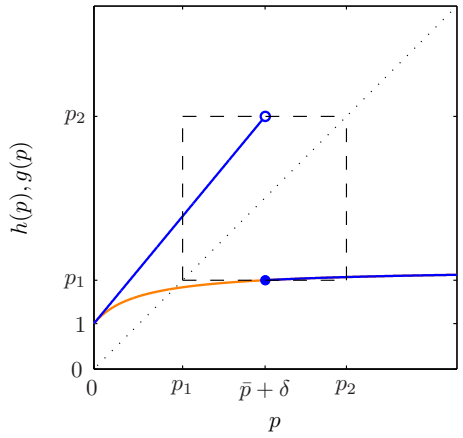

Fig. 5. The functions h (blue) and g (orange). The filled (unfilled) circles indicate a closed (open) interval boundary. The dotted diagonal represents the identity map $p = p$. The intersection of g with the identity diagonal represents the solution $\bar{p}$ to the DARE (6). The dashed box represents the set $[p_1, p_2)$, which is invariant under h. For $p \geq \bar{p} + \delta$, $h(p) = g(p)$.

Proposition 1: Let $p_1 := h(\bar{p}+\delta)$ and $p_2 := a^2(\bar{p}+\delta)+1$. The following properties of h hold:

(i) $h([p_1, p_2)) \subseteq [p_1, p_2)$.
(ii) $\forall p \in [0, \infty), \exists m \in \mathbb{N} : h^m(p) \in [p_1, p_2)$.
(iii) h is injective on $[p_1, p_2)$.
(iv) h is continuous and strictly monotonic increasing on $[p_1, \bar{p} + \delta)$ and on $[\bar{p} + \delta, p_2]$.
(v) h is differentiable on $(p_1, \bar{p} + \delta)$ and on $(\bar{p} + \delta, p_2)$.

For (i), we also say that $[p_1, p_2)$ is an *invariant set under* h.

Proof: The proof can be found in [17]. ■

We are interested in studying convergence of a solution $\{p(0), p(1), p(2), \dots\}$ of (22) to periodic cycles, which can be defined according to [18], as follows:

Definition 1 (adapted from [18]): Let p^* be in the domain of h. Then p^* is called an *N-periodic point* of (22) if it is a fixed point of h^N, that is, if

$$h^N(p^*) = p^*. \tag{26}$$

The periodic orbit of p^*, $\{p^*, h(p^*), h^2(p^*), \dots, h^{N-1}(p^*)\}$, is called an *$N$-cycle*, and N is called the *period*.

Definition 2: A solution to (22) is called *asymptotically N-periodic* if

$$\lim_{m \to \infty} h^{mN}(p_0) = p^*, \tag{27}$$

where p^* is an N-periodic point of (22).

In subsequent sections, we derive conditions that guarantee that a solution to (22) is asymptotically periodic. For this purpose, attention can be restricted to the interval $[p_1, p_2)$, since by Proposition 1, (i) and (ii), every solution enters $[p_1, p_2)$ for some m and remains within for all $k \geq m$.

From Proposition 1, (iii), the inverse of h exists on the range of h on $[p_1, p_2)$, which can be seen from Fig. 5 to be $h([p_1, p_2)) = [p_1, h(p_2)) \cup [h(p_1), p_2)$. Hence, we define the inverse h^{-1} as

$$\begin{aligned} h^{-1} \; &: [p_1, h(p_2)) \cup [h(p_1), p_2) \to [p_1, p_2) \\ &\quad y \;\mapsto\; h^{-1}(y) \text{ such that } h(h^{-1}(y)) = y. \end{aligned} \tag{28}$$

For the domain of h^{-1}, we write $\mathrm{dom}(h^{-1})$.

B. Illustrative example and outline of the proof

We now illustrate, by means of Example 1, the main ideas to show asymptotic periodicity of solutions to (22).

The graph of h for the parameters of Example 1 is shown in Fig. 6. Since there is no intersection with the identity diagonal $p = p$, h has no fixed point, as expected. The graph of h^3, which is depicted in Fig. 7, does, however, have three intersections in $[p_1, p_2)$ with the identity diagonal. Hence, h^3 has three fixed points in this interval corresponding to the 3-cycle shown in Fig. 4(a).

We illustrate next how one can use the contraction mapping theorem to prove that h^3 has these three fixed points, and that they are (locally) attractive. This approach is then generalized in Sec. IV-C to IV-E.

Theorem 1 (Contraction Mapping Theorem, [19]): Let $\|\cdot\|$ be a norm for $\mathbb{R}^n$ and S a closed subset of $\mathbb{R}^n$. Assume $f : S \to S$ is a contraction mapping: there is an L, $0 \leq L < 1$, such that $\|f(p) - f(\tilde{p})\| \leq L\|p - \tilde{p}\|$ for all $p, \tilde{p}$ in S. Then f has a unique fixed point p^* in S. Furthermore, if $p(0) \in S$ and we set $p(k+1) = f(p(k))$, then

$$\|p(k) - p^*\| \leq \frac{L^k}{1 - L}\|p(1) - p(0)\| \quad (k \geq 0). \tag{29}$$

Equation (29) implies that $p(k)$ converges to p^* as $k \to \infty$ for any $p(0) \in S$.

To be able to apply Theorem 1 (with $n = 1$, $f = h^3$, and $\|\cdot\| = |\cdot|$), there are two key requirements:

(i) a suitable closed set S that is invariant under h^3 needs to be constructed, and
(ii) h^3 needs to be a contraction mapping on S.

As it shall be seen later, the discontinuities of the function h^3 play a crucial role in the development. The function h^3 has two discontinuities, which can be seen as follows:

- $h(p)$ is continuous for all $p \in [p_1, p_2)$ except at $d_1 := \bar{p} + \delta$.
- $h^2(p) = h(h(p))$ is continuous at p if h is continuous at p and if h is continuous at $h(p)$, [20]. Hence, points of discontinuity are d_1 (discontinuity of h); and $d_2 \in [p_1, p_2)$ such that $\bar{p} + \delta = d_1 = h(d_2)$. Since $d_1 \in \mathrm{dom}(h^{-1})$, the inverse h^{-1} exists and $d_2 = h^{-1}(d_1)$.
- Similarly, $h^3(p) = h(h^2(p))$ is continuous at p if h^2 is continuous at p and if h is continuous at $h^2(p)$. Points of discontinuity are d_1 and d_2 (discontinuities of h^2); and $d_3 \in [p_1, p_2)$ such that $\bar{p} + \delta = d_1 = h^2(d_3) \Leftrightarrow h^{-1}(d_1) = d_2 = h(d_3)$. But since $d_2 \notin \mathrm{dom}(h^{-1})$ (cf. Fig. 6), such a d_3 does not exist. Hence, h^3 has the discontinuities d_1 and d_2.

The discontinuities d_1 and d_2 naturally subdivide $[p_1, p_2)$ in three disjoint subintervals: $[p_1, p_2) = I_3 \cup I_2 \cup I_1$ with $I_3 := [p_1, d_2)$, $I_2 := [d_2, d_1)$, and $I_1 := [d_1, p_2)$. Figure 8 illustrates where one of the subintervals, I_1, is mapped by repeated application of h. Clearly, $h^3(I_1) = h^3([d_1, p_2)) \subseteq [d_1, p_2) = I_1$. Furthermore, since $h(p_2) < d_2$ (cf. Fig. 6), the same property holds for the closure of I_1; that is, $[d_1, p_2]$ is invariant under h^3,

$$h^3([d_1, p_2]) \subseteq [d_1, p_2]. \tag{30}$$

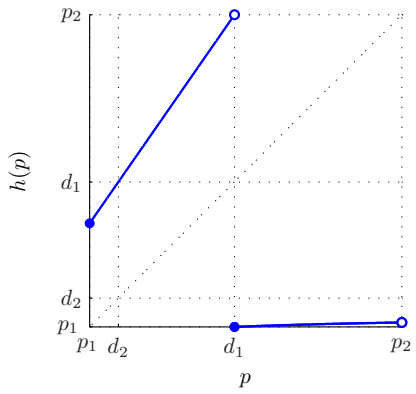

Fig. 6. The function h for $a = 1.2$, $c = 1$, $\delta = 3$ on the domain $[p_1, p_2) = [2.20, 8.13)$. The function has a discontinuity at $d_1 = \bar{p} + \delta = 4.95$. The slope of h is a^2 on (p_1, d_1) and bounded by $g'(d_1)$ on (d_1, p_2).

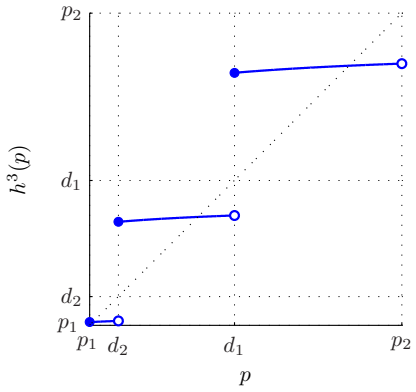

Fig. 7. The function h^3 for $a = 1.2$, $c = 1$, $\delta = 3$ on the domain $[p_1, p_2) = [2.20, 8.13)$. The function has two discontinuities at $d_1 = \bar{p} + \delta = 4.95$ and $d_2 = 2.74$.

Notice that $h([d_1, p_2])$ and $h^2([d_1, p_2])$ (the same intervals as $h(I_1)$ and $h^2(I_1)$ in Fig. 8, but with closed right bounds) are closed intervals contained in I_3 and I_2, respectively. It can be shown that, under h^3, they are invariant and attractive for any point in I_3 and I_2, respectively. Hence, we can construct closed sets invariant under h^3 (requirement (i)).

For requirement (ii), we focus again on the interval I_1. Consider the derivative of h^3 on (d_1, p_2). By the chain rule, for $p \in (d_1, p_2)$,

$$\begin{aligned}\frac{d(h^3)}{dp}(p) &= h'(h^2(p))\,\frac{d(h^2)}{dp}(p)\\ &= h'(h^2(p)) \cdot h'(h(p)) \cdot h'(p), \end{aligned} \tag{31}$$

where h' means $\frac{dh}{dp}$. Similar to the argumentation in Fig. 8, one can see that $h((d_1, p_2)) \subseteq (p_1, d_2)$ and $h^2((d_1, p_2)) \subseteq h((p_1, d_2)) \subseteq (d_2, d_1)$. From Fig. 6, it can be seen that $h'(p) = a^2$ for all $p \in (p_1, d_2) \cup (d_2, d_1)$ and that $h'(p) < g'(d_1)$ for all $p \in (d_1, p_2)$. Therefore, we get[2] from (31), for $p \in (d_1, p_2)$,

$$\frac{d(h^3)}{dp}(p) < a^2 \cdot a^2 \cdot g'(d_1) = a^4 g'(\bar{p} + \delta) = 0.084. \tag{32}$$

[2]The computation is available at www.cube.ethz.ch/downloads.

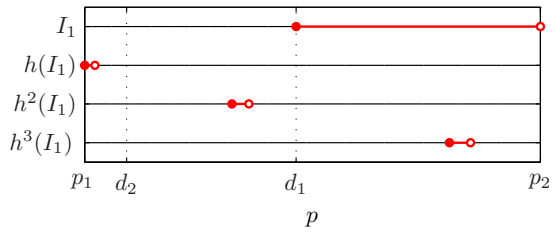

Fig. 8. Mapping of the interval I_1 under repeated application of h. On the top line, the interval $I_1 = [d_1, p_2)$ is shown in red. This interval is mapped to $h(I_1) = [h(d_1), h(p_2)) = [p_1, h(p_2))$ (cf. Fig. 6), shown on the second line from above. Notice that the obtained interval is significantly shorter due to the slope of h being significantly less than one on $[d_1, p_2)$ (cf. Fig. 6). The intervals $h^2(I_1) = h(h(I_1))$ and $h^3(I_1) = h(h^2(I_1))$ (third and fourth line from above) are obtained accordingly. Notice that the interval length increases for the latter two mappings, since the slope of h is greater than one on $[p_1, d_1)$. Still, after one cycle of three mappings, the resulting interval is contained in the original one, i.e. $h^3(I_1) \subseteq I_1$.

From this, it follows (by the application of the mean value theorem, [20]) that for any closed interval $S \subseteq (d_1, p_2)$, the contraction mapping property in Theorem 1 holds with $L = a^4 g'(\bar{p}+\delta) < 1$. Even though the closed interval $[d_1, p_2]$ is not contained in (d_1, p_2), $\tilde{I}_1 := h^3([d_1, p_2])$ *is* contained (see Fig. 8). Furthermore, $\tilde{I}_1$ is itself invariant under h^3, which follows directly from (30),

$$h^3(\tilde{I}_1) = h^3(h^3([d_1, p_2])) \subseteq h^3([d_1, p_2]) = \tilde{I}_1. \tag{33}$$

Theorem 1 thus ensures that there exists a unique fixed point in $\tilde{I}_1$, and that every starting point in $\tilde{I}_1$ converges to this fixed point. Furthermore, since

$$h^3(I_1) = h^3([d_1, p_2)) \subseteq h^3([d_1, p_2]) = \tilde{I}_1, \tag{34}$$

the fixed point is attractive (under h^3) for all points in the original interval I_1.

For the intervals I_2 and I_3, one can proceed similarly and, hence, show that every point in $[p_1, p_2)$ converges to a fixed point of h^3. Furthermore, we know by Proposition 1, (i) and (ii), that every solution to (22) ends up in $[p_1, p_2)$. Therefore, the solution to (22) for the considered example is asymptotically 3-periodic for any initial value p_0.

To treat the general case in the remainder of this section, we proceed analogous to this example. In Sec. IV-C, we state assumptions that guarantee the existence of N closed subintervals in $[p_1, p_2)$ that are invariant under h^N. In Sec. IV-D, we show that h^N is a contraction mapping on these intervals, which then allows us (in Sec. IV-E) to apply Theorem 1 to conclude that solutions to (22) are asymptotically N-periodic.

C. Invariant subintervals

The construction of N closed subintervals of $[p_1, p_2)$ that are invariant under h^N proceeds in two steps. First, half-closed intervals I_i are generated that cover $[p_1, p_2)$ and possess the sought invariance property. Second, closed intervals $\tilde{I}_i \subseteq I_i$ are constructed that inherit the invariance property from their supersets.

Motivated by the example of the previous subsection, the intervals I_i are obtained by splitting up $[p_1, p_2)$ through a

sequence of points $\{d_1, d_2, \dots\}$, $d_i \in [p_1, p_2)$, which represent discontinuities of h^N and are obtained by iteratively applying h^{-1}:

Algorithm 1:

$d_1 := \bar{p} + \delta$
while $d_i \in \text{dom}(h^{-1})$
  $d_{i+1} := h^{-1}(d_i)$
  increment i
end while
$N := i + 1$

If there exists an $m \in \mathbb{N}$ such that $d_m \notin \text{dom}(h^{-1})$, Algorithm 1 terminates, and the obtained sequence $\{d_1, d_2, \dots\}$ is finite. For all problems of an exhaustive search that we have conducted, this has actually been the case. A potential proof that the algorithm terminates in general is, however, still open. For the purpose of this paper, we assume henceforth that it does.

Assumption 1: Algorithm 1 terminates.

The assumption is essentially checked by running Algorithm 1; if the algorithm terminates, the assumption is true.

Proposition 2: Let $\mathcal{D}_i := \{d_1, \dots, d_i\}$. The following statements hold:

(i) $d_i \notin [h(p_2), h(p_1))$, $\forall i < N-1$,
  $d_{N-1} \in [h(p_2), h(p_1))$.
(ii) h^i is continuous on $[p_1, p_2) \setminus \mathcal{D}_i$, $\forall i \leq N-1$,
  h^N is continuous on $[p_1, p_2) \setminus \mathcal{D}_{N-1}$.
(iii) $\forall d_i, d_j \in \mathcal{D}_{N-1}$ with $i \neq j$, $d_i \neq d_j$.

Proof: The proof can be found in [17]. ∎

The points $\mathcal{D}_{N-1}$ divide the interval $[p_1, p_2)$ in N subintervals $\mathcal{I} := \{I_1, \dots, I_N\}$ as illustrated in Fig. 9. The intervals are named such that I_i has d_i as a lower bound for $i \leq N-1$, and I_N has the lower bound p_1. A formal definition of the intervals is given next. Let $\Pi : \{1, \dots, N-1\} \to \{1, \dots, N-1\}$ be a permutation of the d_i's such that

$$d_{\Pi(i)} < d_{\Pi(i+1)}, \quad \forall i \in \{1, \dots, N-2\}. \tag{35}$$

Furthermore, let $\underline{i}$ and $\bar{i}$ be the indices of the smallest and greatest d_i, i.e. $\Pi(1) = \underline{i}$ and $\Pi(N-1) = \bar{i}$. Then define

$$I_i := [d_i, d_{\Pi(\Pi^{-1}(i)+1)}) \quad \forall i \leq N-1, i \neq \bar{i} \tag{36}$$
$$I_{\bar{i}} := [d_{\bar{i}}, p_2) \tag{37}$$
$$I_N := [p_1, d_{\underline{i}}), \tag{38}$$

that is, interval I_i has d_i as a lower bound (closed) and the next bigger element from $\mathcal{D}_{N-1}$ as an upper bound (open) (except for the intervals at the boundaries of $[p_1, p_2)$). Since each interval is uniquely specified from (36)–(38) by either its lower or its upper bound, we sometimes omit either one of them and write $[d, *)$ or $[*, d)$. For the interior (the largest contained open interval) of I_i, we write $\text{int}(I_i)$.

Proposition 3: All intervals $I_i \in \mathcal{I}$ are mutually disjoint and non-empty.

Proof: The proof can be found in [17]. ∎

Proposition 4: The following statements hold:

(i) $h(I_N) \subseteq I_{N-1}$, $h(I_{N-1}) \subseteq I_{N-2}$, …, $h(I_2) \subseteq I_1$, and $h(I_1) \subseteq I_N$.

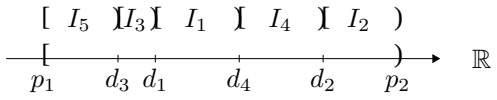

Fig. 9. The left-closed, right-open subintervals $\mathcal{I} = \{I_1, I_2, I_3, I_4, I_5\}$ generated by the points $\mathcal{D}_4 = \{d_1, d_2, d_3, d_4\}$ cover the interval $[p_1, p_2)$.

(ii) $h(\text{int}(I_N)) \subseteq \text{int}(I_{N-1})$, $h(\text{int}(I_{N-1})) \subseteq \text{int}(I_{N-2})$, …, $h(\text{int}(I_2)) \subseteq \text{int}(I_1)$, and $h(\text{int}(I_1)) \subseteq \text{int}(I_N)$.

Proof: The proof can be found in [17]. ∎

Corollary 1: The following statements hold:

(i) $h^N(I_i) \subseteq I_i \;\; \forall I_i \in \mathcal{I}$.
(ii) $h^N(\text{int}(I_i)) \subseteq \text{int}(I_i) \;\; \forall I_i \in \mathcal{I}$.

Proof: (i) and (ii) follow directly from Proposition 4 and the fact: for two sets S_1, S_2 and a function f, $S_1 \subseteq S_2 \Rightarrow f(S_1) \subseteq f(S_2)$. ∎

The intervals $\mathcal{I}$ cover the whole domain of interest $[p_1, p_2)$, and they are invariant under N times application of h. However, in order to be able to apply Theorem 1, closed intervals are required. The proposition below states that subintervals $\tilde{I}_i \subseteq I_i$ exist that are invariant under h^N and closed. For stating the proposition, another technical assumption is required:

Assumption 2: $h(p_2) < d_{N-1}$.

Notice that by Proposition 2, (i), the weaker condition $h(p_2) \leq d_{N-1}$ is already guaranteed.

Proposition 5: There exists a collection of intervals $\tilde{\mathcal{I}} = \{\tilde{I}_1, \tilde{I}_2, \dots, \tilde{I}_N\}$ such that for all $i \in \{1, \dots, N\}$ the following statements hold:

(i) $\tilde{I}_i$ is closed.
(ii) $\tilde{I}_i \subseteq \text{int}(I_i) \subseteq I_i$.
(iii) $h^N(\tilde{I}_i) \subseteq \tilde{I}_i$.
(iv) $h^{2N}(I_i) \subseteq \tilde{I}_i$.

Proof: The proof can be found in [17]. ∎

The details of how the intervals $\tilde{\mathcal{I}}$ can be actually constructed are given in the proof.

D. Contraction mapping

In this section, we show that h^N is a contraction mapping (i.e. it has a Lipschitz constant strictly less than one, cf. Theorem 1) on each of the intervals $\tilde{\mathcal{I}}$. To this end, we first derive an upper bound less than one on the derivative of h^N on the interior of the intervals $\mathcal{I}$.

Proposition 6: h^N is differentiable on all open intervals $\text{int}(I_i)$, $I_i \in \mathcal{I}$. Furthermore, there exists an $L < 1$ such that

$$\left| \frac{d(h^N)}{dp}(p) \right| < L \quad \forall p \in \text{int}(I_i), \forall I_i \in \mathcal{I}.$$

Proof: The proof can be found in [17]. ∎

Corollary 2: h^N is a contraction mapping on any interval of $\tilde{\mathcal{I}}$; that is, there exists an $L < 1$ such that

$$|h^N(p) - h^N(\tilde{p})| \leq L|p - \tilde{p}| \quad \forall p, \tilde{p} \in \tilde{I}_i, \forall \tilde{I}_i \in \tilde{\mathcal{I}}.$$

Proof: Take any $p, \tilde{p} \in \tilde{I}_i$ with $\tilde{p} < p$ without loss of generality. By Proposition 2, (ii), and 5, (ii), h^N is continuous on $[\tilde{p}, p]$ and, by Proposition 6, h^N is differentiable on $(\tilde{p}, p)$.

The claim then follows from the mean value theorem, [20]. (A more detailed proof can be found in [17].) ■

E. Main result

Equipped with the results of the previous two subsections, the main result of this paper can be stated:

Theorem 2: Under Assumptions 1 and 2, the solution to (22) is asymptotically N-periodic for any initial condition $p_0 \geq 0$.

Proof: By Proposition 1, (ii), it follows that there exists an $m_1 \in \mathbb{N}$ such that

$$h^{m_1 N}(p_0) \in [p_1, p_2). \tag{39}$$

Since the disjoint intervals $\mathcal{I}$ cover $[p_1, p_2)$, there exists a unique $i \in \{1, \ldots, N\}$ such that

$$h^{m_1 N}(p_0) \in I_i. \tag{40}$$

By Proposition 5, (iv),

$$h^{(m_1+2)N}(p_0) \in \tilde{I}_i. \tag{41}$$

From Proposition 5, (i) and (iii), Corollary 2, and Theorem 1, it follows that there exists a unique fixed point p_i^* of h^N (hence, an N-periodic point of (22)) in $\tilde{I}_i$ and that, for all $\tilde{p} \in \tilde{I}_i$,

$$\lim_{m\to\infty} h^{mN}(\tilde{p}) = p_i^*. \tag{42}$$

In particular, for $\tilde{p} = h^{(m_1+2)N}(p_0)$ and by (41),

$$\begin{aligned}\lim_{m\to\infty} h^{mN}\big(h^{(m_1+2)N}(p_0)\big) &= \lim_{m\to\infty} h^{(m_1+2+m)N}(p_0) \\ &= \lim_{m\to\infty} h^{mN}(p_0) = p_i^*. \end{aligned} \tag{43}$$

■

V. Discussion

Two assumptions are made to state the main result of this paper in Theorem 2. The question whether the assumptions can be removed is subject to future study. As is, the strength of the result is that it essentially offers a sufficiency test for periodicity (if Algorithm 1 terminates, convergence to a periodic solution with a known period is guaranteed) as an alternative to simulating (1) and having to interpret the result.

This paper deals with the scalar version of the variance iteration of the event-based state estimator with variance-based triggering. Whether the convergence result generalizes to the multi-sensor case (as suggested by the observations in [3]) is an open question.

A periodic solution to the event-based state estimation problem with variance-based triggering allows the recovery of a time-based transmit schedule: the periodic transmit sequence can be implemented on a sensor as a time-based schedule, which reduces the computational requirements on the sensor. The rate of the time-based transmission is, however, not a design parameter, but obtained from an event-based approach, where the designer specifies tolerable bounds on the estimation variance. Hence, the methods presented herein and in [3] for the multi-sensor case can be used as a tool for designing sensor update rates in an NCS.

VI. Acknowledgments

This work was funded by the Swiss National Science Foundation (SNSF).

References

[1] "Balancing Cube website," [accessed 13.08.2012]. [Online]. Available: http://www.cube.ethz.ch

[2] S. Trimpe and R. D'Andrea, "An experimental demonstration of a distributed and event-based state estimation algorithm," in *Proc. of the 18th IFAC World Congress*, Milano, Italy, Aug. 2011, pp. 8811–8818.

[3] ——, "Reduced communication state estimation for control of an unstable networked control system," in *Proc. of the 50th IEEE Conference on Decision and Control and European Control Conference*, Orlando, FL, USA, 2011, pp. 2361–2368.

[4] M. Lemmon, "Event-triggered feedback in control, estimation, and optimization," in *Networked Control Systems*, ser. Lecture Notes in Control and Information Sciences, A. Bemporad, M. Heemels, and M. Johansson, Eds. Springer Berlin / Heidelberg, 2011, vol. 406, pp. 293–358.

[5] O. Imer and T. Basar, "Optimal estimation with limited measurements," in *Proc. of the 44th IEEE Conference on Decision and Control and the European Control Conference*, Dec. 2005, pp. 1029–1034.

[6] L. Li, M. Lemmon, and X. Wang, "Event-triggered state estimation in vector linear processes," in *Proc. of the American Control Conference*, Jul. 2010, pp. 2138–2143.

[7] M. Rabi, G. Moustakides, and J. Baras, "Multiple sampling for estimation on a finite horizon," in *Proc. of the 45th IEEE Conference on Decision and Control*, Dec. 2006, pp. 1351–1357.

[8] Y. Xu and J. Hespanha, "Estimation under uncontrolled and controlled communications in networked control systems," in *Proc. of the 44th IEEE Conference on Decision and Control and the European Control Conference*, Seville, Spain, Dec. 2005, pp. 842–847.

[9] R. Cogill, S. Lall, and J. Hespanha, "A constant factor approximation algorithm for event-based sampling," in *Proc. of the American Control Conference*, Jul. 2007, pp. 305–311.

[10] J. Sijs and M. Lazar, "On event based state estimation," in *Hybrid Systems: Computation and Control*, ser. Lecture Notes in Computer Science, R. Majumdar and P. Tabuada, Eds. Springer Berlin / Heidelberg, 2009, vol. 5469, pp. 336–350.

[11] J. Sijs, M. Lazar, and W. P. M. H. Heemels, "On integration of event-based estimation and robust MPC in a feedback loop," in *Proc. of the 13th ACM international conference on hybrid systems: computation and control*, New York, NY, USA, 2010, pp. 31–40.

[12] J. Weimer, J. Araujo, and K. H. Johansson, "Distributed event-triggered estimation in networked systems," in *Proc. of the 4th IFAC conference on Analysis and Design of Hybrid Systems*, Eindhoven, Netherlands, Jun. 2012, pp. 178–185.

[13] H. Sandberg, M. Rabi, M. Skoglund, and K. H. Johansson, "Estimation over heterogeneous sensor networks," in *Proc. of the 47th IEEE Conference on Decision and Control*, Cancun, Mexico, Dec. 2008, pp. 4898–4903.

[14] B. D. O. Anderson and J. B. Moore, *Optimal Filtering*. Mineola, New York: Dover Publications, 2005, originally published by Prentice-Hall 1979.

[15] S. Bittanti, P. Colaneri, and G. De Nicolao, "The difference periodic Riccati equation for the periodic prediction problem," *IEEE Transactions on Automatic Control*, vol. 33, no. 8, pp. 706–712, Aug. 1988.

[16] B. Sinopoli, L. Schenato, M. Franceschetti, K. Poolla, M. Jordan, and S. Sastry, "Kalman filtering with intermittent observations," *IEEE Transactions on Automatic Control*, vol. 49, no. 9, pp. 1453–1464, Sep. 2004.

[17] S. Trimpe and R. D'Andrea, "Addendum to: Event-based state estimation with variance-based triggering," IDSC, ETH Zürich, Tech. Rep., 2012. [Online]. Available: http://www.cube.ethz.ch/downloads

[18] S. Elaydi, *An Introduction to Difference Equations*, 3rd ed., ser. Undergraduate Texts in Mathematics, S. Axler, F. W. Gehring, and K. A. Ribet, Eds. Springer New York, 2005.

[19] W. G. Kelley and A. C. Peterson, *Difference equations: an introduction with applications*. San Diego, USA: Academic Press, Inc., 1991.

[20] W. Rudin, *Principles of Mathematical Analysis*, 3rd ed. McGraw-Hill, 1976.